


RESEARCH PAPER

Cyclic-AMP signalling, MYC and hypoxia-inducible factor 1 α intersect to regulate angiogenesis in B-cell lymphoma

Purushoth Ethiraj¹ | Binu Sasi¹ | Kenneth N. Holder² | An-Ping Lin¹ | Zhijun Qiu¹ | Carine Jaafar¹ | Alia Elkhaili¹ | Parth Desai³ | Annapurna Saksena² | Jacob P. Ritter² | Ricardo C. T. Aguiar^{1,4} 

¹Division of Hematology and Medical Oncology, Department of Medicine, University of Texas Health Science Center San Antonio, San Antonio, Texas, USA

²Department of Pathology, University of Texas Health Science Center San Antonio, San Antonio, Texas, USA

³Department of Medicine, University of Texas Health Science Center San Antonio, San Antonio, Texas, USA

⁴South Texas Veterans Health Care System, Audie Murphy VA Hospital, San Antonio, Texas, USA

Correspondence

Ricardo C. T. Aguiar, Department of Medicine, UT Health Science Center San Antonio, San Antonio, TX, USA.
 Email: aguiarr@uthscsa.edu

Funding information

National Institute of General Medical Sciences, Grant/Award Number: R01-GM140456; Leukaemia and Lymphoma Society, Grant/Award Number: TRP-6524-17; Cancer Prevention and Research Institute of Texas, Grant/Award Number: RP170146; National Institute of Environmental Health Sciences, Grant/Award Number: R01-ES031522; Veterans Administration, Grant/Award Number: I01BX001882

Summary

Angiogenesis and MYC expression associate with poor outcome in diffuse large B-cell lymphoma (DLBCL). MYC promotes neo-vasculature development but whether its deregulation in DLBCL contributes to angiogenesis is unclear. Examination of this relationship may uncover novel pathogenic regulatory circuitry as well as anti-angiogenic strategies in DLBCL. Here, we show that MYC expression positively correlates with vascular endothelial growth factor (VEGF) expression and angiogenesis in primary DLBCL biopsies, independently of dual expressor status or cell-of-origin classification. We found that MYC promotes VEGFA expression, a correlation that was validated in large datasets of mature B-cell tumours. Using DLBCL cell lines and patient-derived xenograft models, we identified the second messenger cyclic-AMP (cAMP) as a potent suppressor of MYC expression, VEGFA secretion and angiogenesis in DLBCL in normoxia. In hypoxia, cAMP switched targets and suppressed hypoxia-inducible factor 1 α , a master regulator of VEGFA/angiogenesis in low oxygen environments. Lastly, we used the phosphodiesterase 4b (Pde4b) knockout mouse to demonstrate that the cAMP/PDE4 axis exercises additional anti-angiogenesis by directly targeting the lymphoma microenvironment. In conclusion, MYC could play a direct role in DLBCL angiogenesis, and modulation of cAMP levels, which can be achieved with clinical grade PDE4 inhibitors, has cell and non-cell autonomous anti-angiogenic activity in DLBCL.

KEYWORDS

angiogenesis, cyclic-AMP, hypoxia, lymphoma, MYC

INTRODUCTION

Angiogenesis is a poor prognostic feature of diffuse large B-cell lymphoma (DLBCL).^{1–3} Attempts to address this association by adding bevacizumab to R-CHOP (rituximab-cyclophosphamide, doxorubicin, vincristine [Oncovin] and prednisone) resulted in cardiotoxicity and did not improve

survival of patients with DLBCL.⁴ Also, despite extensive examination of the mutational landscape of DLBCL,⁵ a robust link between the genetic makeup of the lymphoma cells and a pro-angiogenic lymphoma microenvironment is not apparent.

Deregulation of MYC is common to many cancers, and a hallmark of B-cell lymphoma.⁵ The contribution of MYC

Purushoth Ethiraj, Binu Sasi and Kenneth N. Holder have equal contribution.

© 2022 British Society for Haematology and John Wiley & Sons Ltd.

to lymphomagenesis is multiple; it drives a gene expression profile that promotes cell growth, proliferation and rewires metabolism.⁶ In various model systems, MYC is a central regulator of angiogenesis, in part by promoting vascular endothelial growth factor (VEGF) secretion in the tumour microenvironment (TME).⁷ However, the relationship between MYC expression and the degree of angiogenesis in DLBCL remains underexplored.

Recently, we reported that the second messenger, cyclic-AMP (cAMP), inhibits lymphoma angiogenesis in a phosphodiesterase 4 (PDE4)-regulated manner.⁸ This observation agreed with the role of PDE4 as the principal regulator of cAMP hydrolysis in lymphocytes.⁹ In an unrelated work, it was shown that cAMP suppresses MYC transcription in DLBCL.¹⁰ These data attracted our attention because of the putative role of MYC in DLBCL angiogenesis, and the possibility that cAMP may suppress MYC's pro-angiogenic signals.

The pathways and outputs influenced by cAMP are wide-ranging.⁹ In fact, considering exclusively angiogenesis, in addition to the interactions reported earlier between cAMP and phosphatidylinositol-3 kinase (PI3K)/protein kinase B (AKT)/VEGFA,⁸ cAMP has also been reported to inhibit hypoxia-inducible factor-1 α (HIF1 α) and HIF2 α transcription, an essential regulatory node for the secretion of pro-angiogenic factors that forms the basis for the adaptive behaviour of tumour cells under hypoxia.^{11,12} Lastly, in non-tumoural models, cAMP is known to directly inhibit endothelial cells.^{13–16}

Here, to address the potential relationship between MYC expression and angiogenesis in DLBCL, and the intersection between cAMP and angiogenic signals derived from MYC and HIF, we examined DLBCL biopsies, B-cell models of inducible MYC, DLBCL cell lines, patient-derived xenografts (PDXs) and genetically engineered mouse models of lymphoma.

MATERIAL AND METHODS (SEE ALSO SUPPLEMENTARY MATERIAL AND METHODS)

Cell lines and primary tumour samples

The DLBCL cell lines (SU-DHL2, SU-DHL4, SU-DHL6, SU-DHL8, SU-DHL10, OCI-Ly1, OCI-Ly3, OCI-Ly10, RIVA), and MYC-regulatable P493-6 cells were cultured as previously described.¹⁷ The PDXs were obtained from the public repository of xenografts (<https://www.proxe.org/>) and expanded in a local colony of NSG (non-obese diabetic [NOD]-severe combined immunodeficiency [SCID] gamma) mice, as reported.¹⁸ Cell lines and PDXs were examined in normoxia or hypoxia (5% O₂), as described.¹⁹ Clustered regularly interspaced short palindromic repeats (CRISPR) knockouts (KOs) were generated as we previously described.²⁰ Formalin-fixed paraffin-embedded blocks were available from 56 biopsies

of untreated patients with DLBCL, obtained de-identified from our Department of Pathology and University Hospital System. Their use was approved by the Institutional Review Board of University of Texas Health Science Center at San Antonio (UTHSCSA).

Mice – adoptive transfer assays

The Pde4b^{-/-}; E μ -Myc⁻ mice were previously described.⁸ Upon lymphoma development, mice were humanely killed and enlarged lymph nodes harvested, as we previously described.²¹ Cohorts of 6–8-week-old Pde4b wild-type (WT) or Pde4b^{-/-} mice were transplanted with lymphoma cells (1 \times 10⁶ cells, tail vein) from tumours that developed in Pde4b^{+/+} or Pde4b^{-/-} E μ -Myc mice. Experimental procedures were approved by the Institutional Animal Care and Use Committee of the UTHSCSA.

Immunoblotting analysis

Whole-cell lysates were immunoblotted for c-MYC (clone 9E10), HIF1 α (clone 54), HIF2 α (clone D9E3) and anti- β -Actin (Clone AC-74), as described.²²

Histopathology

Slides stained for CD34 were digitally scanned and examined in a blinded fashion by three pathologists (K.N.H., P.D., A.S.) for microvessel density (MVD) quantification using Aperio ImageScope software (Leica Biosystems). For each case, three 'hot spots' (area of maximal MVD) were examined and all microvessels manually counted and highlighted using the ImageScope software, which calculated the area of each vessel, defined as the sum of all microvessel areas divided by the total area analysed (three hot spots = 3.42 mm²) as we described.⁸ Human DLBCL were also stained for MYC, VEGF, BCL2, CD10, BCL6, multiple myeloma oncogene 1 (MUM1, IRF4), MYC and BCL2 were scored semi-quantitatively with cut-off values of 40% and 50% respectively²³; VEGF intensity was scored on 0–3 scale. The DLBCLs were classified as germinal centre B-cell like (GCB) or non-GCB using cut-off values of 30% for CD10, BCL6 and MUM1.²⁴

Statistical analysis

The *p* values were calculated using the Student's *t*-test (two-tailed, equal variance) or the unpaired non-parametric Mann–Whitney test (two-tailed), the Spearman test was used to estimate correlation; all tests were performed with GraphPad Prism 8 software. A *p* \leq 0.05 was considered significant.

RESULTS

MYC expression positively correlates with MVD in DLBCL biopsies

MYC expression, especially in the context of BCL2 co-expression, is associated with poor DLBCL outcome.^{25–27} A high degree of angiogenesis in the DLBCL microenvironment also negatively influences DLBCL survival.^{1,2,28,29} To examine the potential correlation between these biological markers, we performed immunohistochemistry (IHC) for MYC, BCL2 and CD34 in 56 DLBCL biopsies (Table S1). Although not exclusively expressed in endothelial cells, CD34 is a robust, commonly used, marker for vessel quantification in B-cell lymphomas^{29–34} (see Methods S1, and our earlier report,⁸ for detailed validation of this staining strategy). MVD quantification was performed as we previously reported⁸ (see Methods S1 for details); the cut-off for MYC and BCL2 positive biopsies, was $\geq 40\%$ and $\geq 50\%$ respectively. MVD and MYC were quantified in all 56 tumours and BCL2 in 51. Using the Han's classifier,²⁴ 51 tumours were defined as either GCB ($n = 30$) or non-GCB ($n = 21$). About one-third of the DLBCLs were MYC positive (19 of 56), over half were BCL2 positive (27 of 51) and 11 of 51 were double expressers (DE, MYC and BCL2 positive). MYC-positive DLBCLs had significantly higher MVD, while MVD was not different in BCL2-positive or -negative tumours (Figure 1A, Figure S1A). In addition, in this series, the degree of angiogenesis in the TME was not significantly

different between GCB or non-GCB, nor between DE or non-DE DLBCLs (irrespective of the MYC status of the non-DE tumours) (Figure S1B–D). Notably, even after removing the DE DLBCLs from the MYC-positive cohort, the influence of MYC expression on MVD was still present (Figure 1B). Examining the expression of MYC as continuous variable, instead of the dichotomised positive and negative biopsies, confirmed the correlation ($r = 0.42$, Spearman correlation, $p < 0.01$) between MYC expression and angiogenesis (Figure 1C). We concluded that MYC, independently of BCL2 co-expression, or the cell-of-origin classification, is a correlative marker of angiogenesis in DLBCL.

Regulation of VEGFA may contribute to MYC pro-angiogenic role in B-cell malignancies

An interplay between MYC and VEGF has been reported.⁷ To confirm the relevance of these interactions, we used the human B-cell line P493-6, which has MYC expression under the control of a tetracycline-responsive element. Abolishing MYC expression in P493-6 cells significantly suppressed VEGFA secretion as well as its transcription (Figure 2A). We expanded this observation to in vivo models and investigated the expression and secretion of VEGFA in mature B cells from 8 to 12 weeks old, lymphoma-free, E μ -MYC and WT mice. We found increased VEGFA transcription and secretion in B lymphocytes from E μ -MYC mice (Figure 2B). Next, we used an in silico approach to

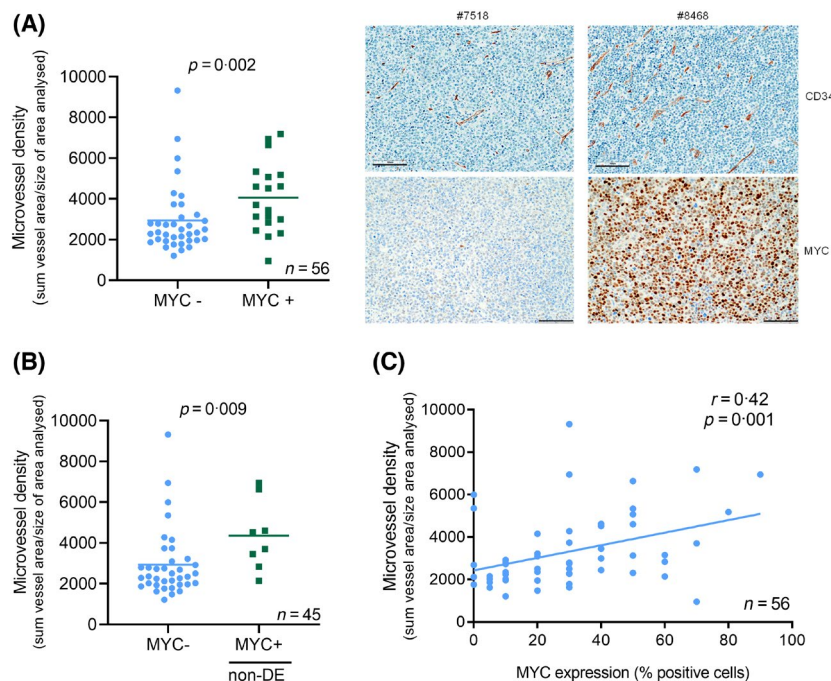


FIGURE 1 MYC expression and microvessel density (MVD) in diffuse large B-cell lymphoma (DLBCL). (A) Vessel area in MYC-positive and -negative DLBCLs; right panel shows representative immunohistochemistry of MYC-positive/high MVD (CD34 staining) and MYC-negative/low MVD DLBCLs. The size bar indicates 100 μ m. (B) Vessel area in MYC-negative and MYC-positive DLBCLs excluding double MYC/BCL2 expressors (DE). (C) Linear regression analysis between MVD and MYC expression in 56 primary human DLBCLs (Spearman's correlation coefficient $r = 0.42$, $p = 0.001$). The p values in (A) and (B) are from non-parametric Mann–Whitney tests

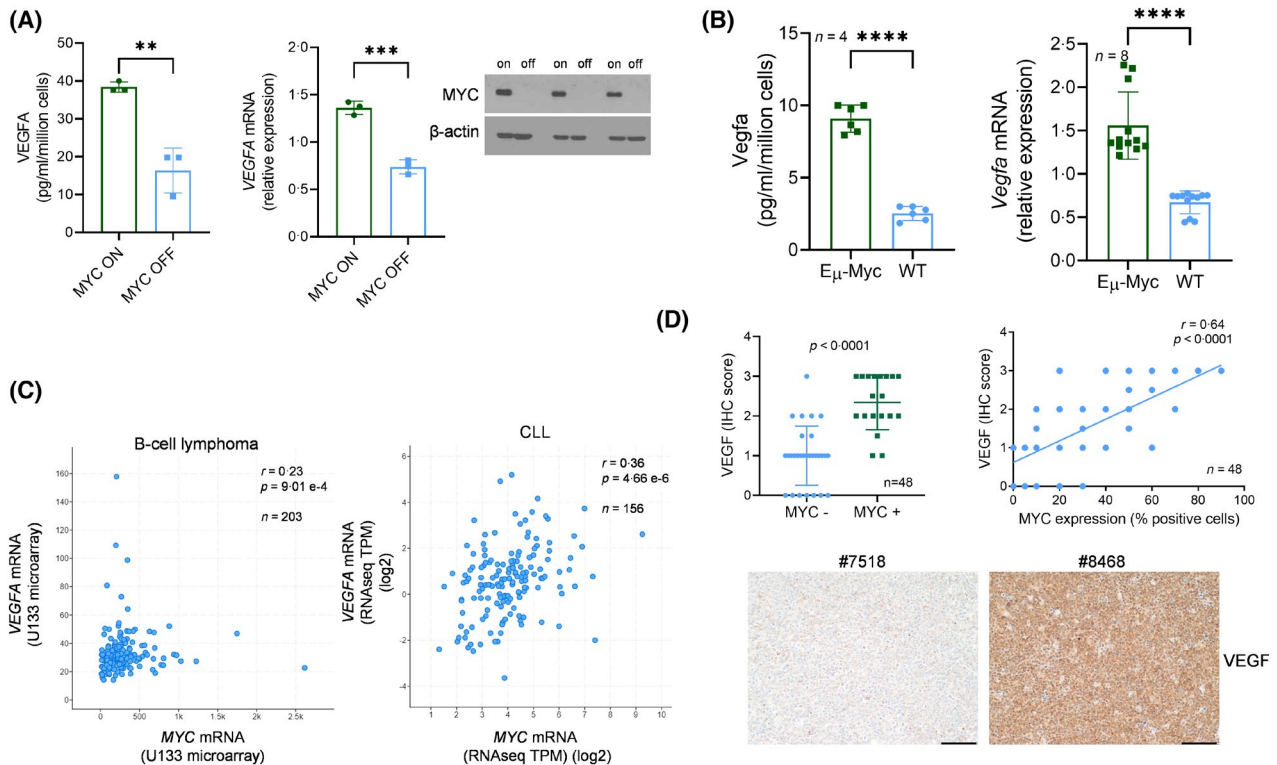


FIGURE 2 MYC and vascular endothelial growth factor A (VEGFA) expression in malignant mature B cells. (A) Left to right – VEGFA secretion (enzyme-linked immunosorbent assay [ELISA] – conditioned media) and mRNA expression in P493-6 cells with or without MYC expression. Data are mean and SD from three biological replicates – Western blot (WB) for MYC expression is shown to the right. (B) Left to right – VEGFA secretion (ELISA – conditioned media) and mRNA expression in mature B cells from E μ -Myc and wild-type (WT) mice. Data are mean and SD from four (ELISA) and eight (quantitative reverse transcription polymerase chain reaction) mice, all analysed in triplicate. (C) Correlation between VEGFA and MYC mRNA expression in 203 B-cell lymphomas and 156 chronic lymphocytic leukaemia samples (Spearman's correlation coefficient $r = 0.23$, $p = 9.01 \text{ e-}4$ and $r = 0.36$, $p = 4.66 \text{ e-}6$, respectively). (D) Left panel - VEGF expression in MYC-negative and -positive diffuse large B-cell lymphomas (DLBCLs); right panel - linear regression analysis between VEGF and MYC expression in 48 human DLBCLs (Spearman's correlation coefficient $r = 0.64$, $p < 0.0001$). Lower panel shows representative immunohistochemistry of VEGF low and high biopsies (same tumours as in Figure 1A). The size bar indicates 100 μm . The p values in (A) and (B) are from two-sided Student's t -tests, ** <0.01 , *** <0.001 , **** <0.0001 ; the p values in (D) are from non-parametric Mann-Whitney tests

examine the CHIP-seq Clusters function of ENCODE (encodeproject.org) and confirmed that MYC binds to the canonical CACGTG motif in multiple areas of the regulatory region of VEGFA (Figure S2A). These results led us to explore the relationship between MYC and VEGFA in cancer datasets (cbioportal.org).³⁵ Analysis of B-cell lymphomas ($n = 203$), and of the related mature B-cell malignancy chronic lymphoid leukaemia ($n = 156$), confirmed a significant, although modest, correlation between MYC and VEGFA expression ($r = 0.23$, $r = 0.36$, respectively, Spearman test, $p < 0.0001$) (Figure 2C). Finally, we went back to the primary DLBCL biopsies and quantified VEGF expression using IHC. We found that MYC-positive DLBCLs expressed VEGF at significantly higher levels than MYC-negative tumours, and that a significant positive correlation between MYC and VEGF levels was present when MYC expression was considered as a continuous variable, instead of dichotomised into positive and negative ($R = 0.64$, Spearman test, $p < 0.0001$, Figure 2D). We concluded that heightened angiogenesis in mature B-cell malignancies may include the co-ordinated contribution of MYC and VEGF.

Cyclic-AMP suppresses MYC, VEGFA and angiogenesis in DLBCL

We showed earlier that the cAMP-PDE4B axis influences angiogenesis in DLBCL.⁸ Recently, a regulatory circuitry involving cAMP and MYC expression was reported in B-cell lymphoma.¹⁰ Thus, we hypothesised that cAMP may be an upstream signal that modulates MYC effects towards VEGFA and angiogenesis. To explore this possibility, we used a combination of forskolin (an adenylyl cyclase activator) and roflumilast (a United States Food and Drug Administration [FDA]-approved PDE4 inhibitor) to modulate intracellular cAMP levels in DLBCL cell lines and PDX models, and quantified MYC expression and VEGFA secretion. It should be noted, as we and others reported earlier,^{10,36-39} that at baseline DLBCL models display nearly undetectable levels of cAMP, due to the low basal activity of adenylyl cyclase. Therefore, to uncover the role of PDE4, which functions exclusively to hydrolyse cAMP,⁹ it is essential that the intracellular levels of this second messenger be first elevated with forskolin; only then inhibiting PDE4, with roflumilast, would be of

relevance. Here, in agreement with this well-established concept, the combination of forskolin and roflumilast (i.e., cAMP elevation) induced MYC suppression and a decrease in VEGFA secretion (Figure 3A,B), while single agents had limited activity (Figure S3A). The effects of forskolin and roflumilast towards MYC and VEGFA in cell lines were validated in six independent DLBCL PDX models analysed ex vivo (Figure 3C,D, Figure S3B). We also demonstrated that suppression of MYC and VEGFA that followed elevation of cAMP levels occurred at the

RNA level (Figure S3C,D), in agreement with earlier reports.^{7,10} Next, we performed human umbilical vein endothelial cells (HUVEC) tube formation assays to test if the degree of suppression of VEGFA secretion by the lymphoma cells was functionally relevant. We detected significantly decreased number of branch points, loops, and tube length formed by these endothelial cells grown in conditioned media from isogenic cAMP-high versus cAMP-low DLBCL models, a phenotype that was rescued by the addition of recombinant human VEGFA

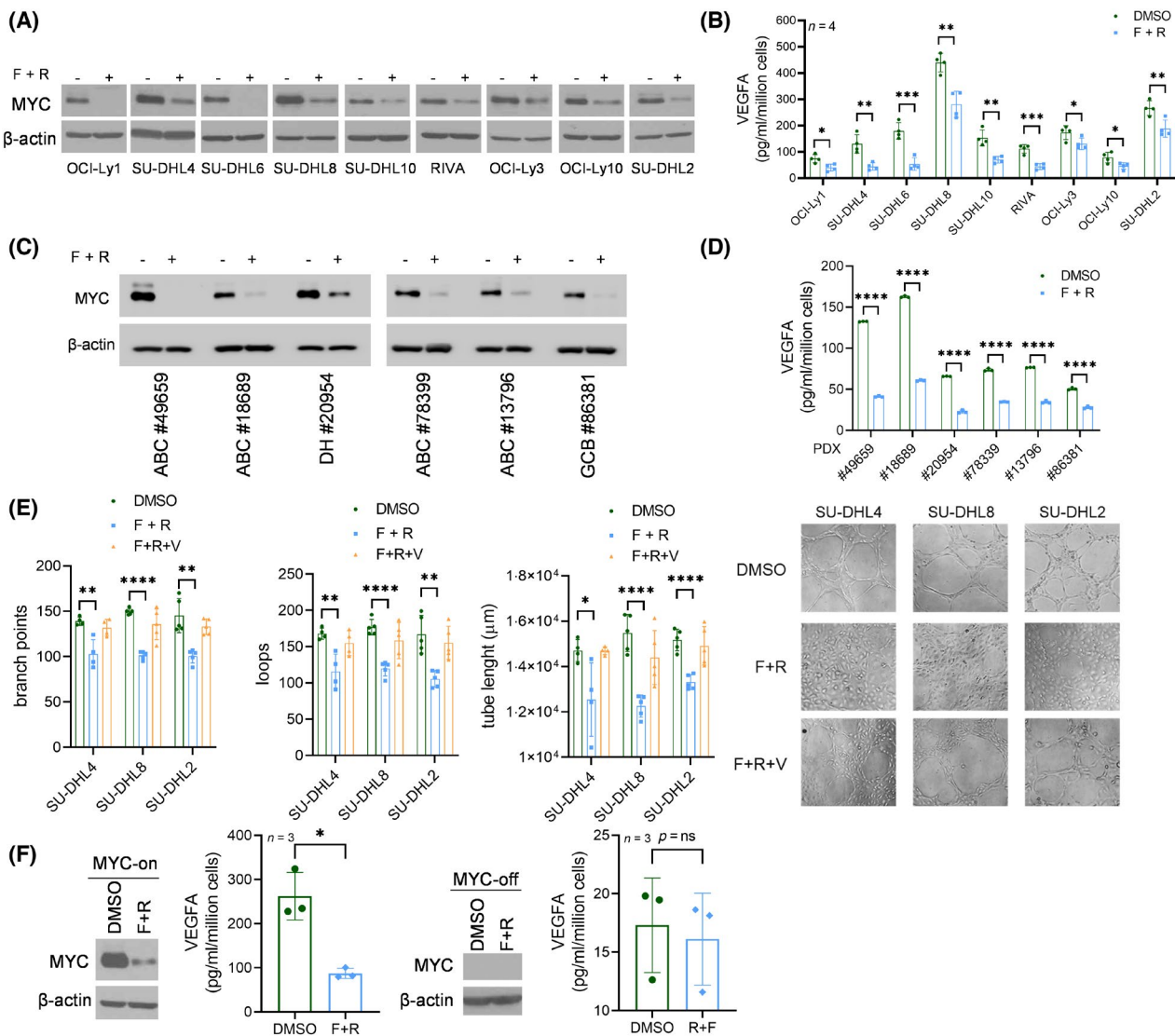


FIGURE 3 Cyclic-AMP modulation of MYC and vascular endothelial growth factor A (VEGFA) in B-cell lymphomas. (A) MYC protein expression (Western blot [WB]) in diffuse large B-cell lymphoma (DLBCL) cell lines exposed to forskolin (40 μ M) and roflumilast (10 μ M) (F + R) or vehicle control (dimethyl sulphoxide [DMSO]) for 16 h. (B) VEGFA secretion (enzyme-linked immunosorbent assay [ELISA] – conditioned media) of DLBCL cell lines exposed to F + R or DMSO for 16 h. Data are mean \pm SD from four biological replicates. (C) MYC protein expression (WB) in DLBCL patient-derived xenografts (PDXs) exposed to F + R or DMSO for 16 h. (D) VEGFA secretion (ELISA – conditioned media) of DLBCL PDX models exposed to F + R or DMSO for 16 h. Data are mean \pm SD of three technical replicates – additional biological replicates are shown in Figure S3B. (E) Tube-forming capacity of human umbilical vein endothelial cells (HUVEC, number of branch points, loops and tube length – Left to right) grown in conditioned media DLBCL cell lines exposed to DMSO, F + R, or F + R supplemented with recombinant VEGFA (50 ng/ml, F + R + V). Data shown are the mean \pm SD from four to five replicates quantified using image J software. Representative tube formation images are shown to right of the graphs. (F) MYC expression (WB) and VEGFA secretion (ELISA) in P493-6 MYC ON (left panels) or MYC OFF (right panels) exposed to F + R for 16 h. Data are mean \pm SD from three biological replicates. All *p* values are from two-sided Student's *t*-tests, **p* < 0.05, ***p* < 0.01, ****p* < 0.001, *****p* < 0.0001. In (E), the differences between DMSO and F + R + V are not significant

(Figure 3E). Lastly, to determine if MYC was mediating the suppressive effects of cAMP towards VEGFA, we returned to the MYC-regulatable P493-6 cells. We showed that the combination of forskolin and roflumilast readily suppressed VEGFA in MYC-ON cells, in association with MYC downregulation, but it did not modify VEGFA levels if MYC expression was turned OFF in the isogenic P493-6 model (Figure 3F). We concluded that cAMP downregulates MYC/VEGFA axis in DLBCL and possibly angiogenesis in the lymphoma microenvironment. The mechanism by which the transcription of ectopic MYC in P493-6 cells is downmodulated by cAMP remains to be defined, but it does not include change in mRNA stability (Figure S3E,F).

The cAMP-PDE4 axis suppresses HIF1 α and hypoxia-mediated VEGFA secretion

A cross-talk between the cAMP-PDE4 axis and HIF signalling, one of the most potent regulators of VEGF transcription, secretion, and ultimately angiogenesis, has been suggested in non-cancer models and shown to be cell-type specific.^{11,12} Here, we explored the potential role of cAMP in controlling HIF signals in DLBCL. To that end, we exposed 15 unique DLBCL models (nine cell lines, six PDXs) to hypoxia (5% O₂) for 16h and quantified HIF1 α and HIF2 α by Western blot. HIF1 α was induced by hypoxia in all but one (SU-DHL8) of the models examined (Figure 4A,B). In a fraction of the cell lines (five of nine), but in none of the PDXs, HIF1 α was already detected in normoxia, albeit still readily inducible by hypoxia. Conversely, HIF2 α was not expressed in DLBCL, in normoxia or hypoxia (Figure S4A,B). Notably, in nearly all models investigated (eight of nine cell lines and all PDXs), the combination of forskolin and roflumilast suppressed HIF1 α expression in hypoxia and/or normoxia (Figure 4A,B); note that in SU-DHL8 and OCI-Ly10 the inhibition of HIF1 α is detected only in normoxia (in these two cell lines, as well as SU-DHL4, a modest increase in HIF1 α is detected following exposure to F + R in hypoxia). More importantly, additional investigation showed that cAMP suppressed HIF1 α in DLBCL at transcriptional level (Figure S4C).

Hypoxia, in a HIF-dependent manner, has been previously reported to promote MYC degradation in epithelial cell models.^{40,41} We found that hypoxia also suppressed MYC expression in DLBCL (Figure 4A,B, compare lanes 1 and 3), and that exposure to forskolin and roflumilast appeared to further MYC downregulation in hypoxia (Figure 4A – compare lanes 3 and 4). These data suggest that cAMP may suppress two VEGF-inducing pro-angiogenic nodes, HIF1 α and MYC. To confirm this assertion, we first measured VEGFA in the cell lines and PDX DLBCL models in normoxia or hypoxia (5% O₂ for 16h). In all instances, expectedly, hypoxia increased VEGFA levels (cell lines: mean 2.9-fold increase, range 1.9–5.04 PDX: mean 3.1-fold increase, range 2.2–4.5,

Figure S4D), while cAMP significantly suppressed VEGFA in hypoxia (Figure 4C,D, Figure S4E), which we postulated derived at least in part from the downregulation of HIF1 α (and attendant effects in its direct target, VEGFA). In agreement with this concept, we detected cAMP-mediated transcriptional downregulation of additional HIF1 α targets (BCL2 interacting protein 3 (BNIP3), carbonic anhydrase 9 (CAIX), Egl-9 family hypoxia inducible factor 1 (EGLN1)] in multiple DLBCL models (Figure S4F). We also confirmed that hypoxia per se does not modify the intracellular levels of cAMP, and that forskolin and roflumilast upregulated the levels of this second messenger to the same extent in normoxia and hypoxia (Figure S4G). Next, to further investigate the relationship between HIF1 α and MYC during hypoxia in DLBCL, we generated CRISPR-based HIF1 α KO in the DLBCL cell line SU-DHL10. Examination of HIF1 α KO clones unexpectedly revealed that contrary to epithelial cells,^{40,41} in this DLBCL model MYC downregulation in hypoxia is HIF1 α independent, as it occurred to a similar degree in HIF1 α WT or KO cells (Figure 4E). We also verified that in the HIF1 α -KO cells there was no change in HIF2 α expression, which remained undetectable, mitigating concerns of a potential confounding effect from HIF2 α on MYC suppression (Figure S4H). This DLBCL KO model was also used to strengthen the concept that HIF1 α is mediating at least part of the cAMP suppressive effects on VEGFA expression. Quantification of VEGFA in these cells showed that in a HIF1 α WT status, cAMP suppressed all VEGFA induced by hypoxia, which is a significantly larger amount than that generated by HIF1 α KO cells in hypoxia. In other words, there is a more pronounced cAMP-mediated ‘clearance’ of VEGFA (in pmol/million cells) in HIF1 α WT than KO cells (Figure 4E, Figure S4I). Importantly, this response could be more confidently ascribed to cAMP effects towards HIF1 α because the confounding cAMP-mediated MYC suppression during hypoxia was equally present in HIF1 α -WT and -KO cells (Figure 4E). Finally, this genetic loss-of-function model was cross-validated by a pharmacological approach to stabilise HIF1 α . In brief, DLBCL cell lines were exposed to the prolyl hydroxylase (PHD) inhibitor molidustat in presence or absence of forskolin and roflumilast (cAMP), and HIF1 α , MYC and VEGFA expression quantified. Pharmacological stabilisation of HIF1 α protein by molidustat blunted cAMP effects towards VEGFA (Figure 4F, Figure S4J). In these assays, we detected only ~20% suppression of VEGFA by cAMP versus ~80% suppression during hypoxia, wherein, differently from the molidustat-treated cells, cAMP also markedly inhibited HIF1 α expression (Figure 4A,C). Analysis of MYC in this model was also informative; first, it showed that HIF1 α expression/stabilisation alone does not suppress MYC, validating the HIF1 α KO data and strongly suggesting that in DLBCL MYC suppression during hypoxia is HIF1 α independent. In addition, as cAMP readily suppressed MYC in molidustat-treated cells, the limited downmodulation of VEGFA in these cells further support the idea that HIF1 α is mediating at least part of the cAMP effects towards VEGFA expression.

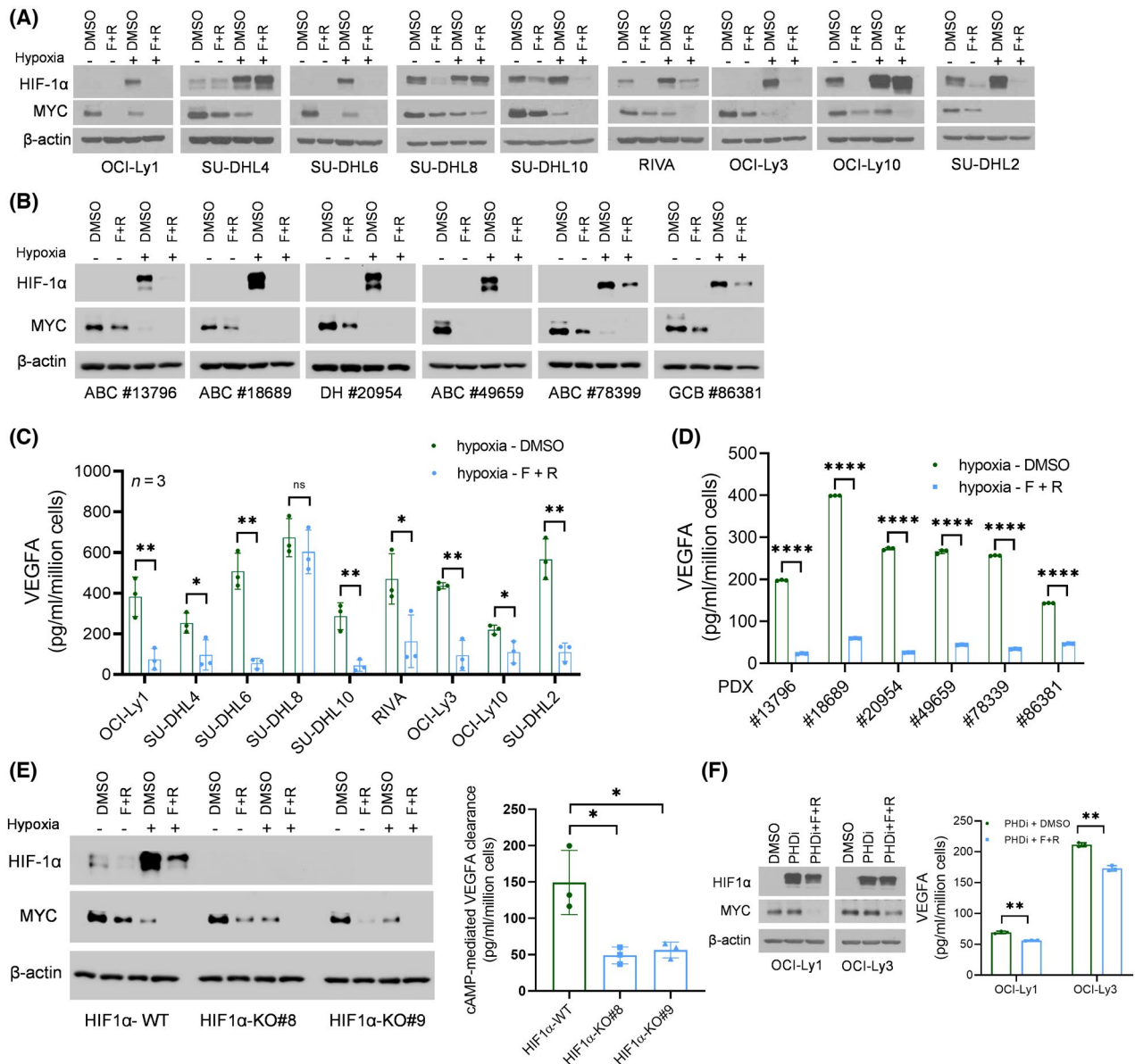


FIGURE 4 Cyclic-AMP modulation of MYC, hypoxia-inducible factor 1 α (HIF1 α) and vascular endothelial growth factor A (VEGFA) in diffuse large B-cell lymphoma (DLBCL). (A) Western (WB) analysis of HIF1 α and MYC protein expression in DLBCL cell lines grown in normoxia (21% O₂) or hypoxia (5% O₂) for 16h and exposed to dimethyl sulphoxide (DMSO) or forskolin and roflumilast (F+R, 40 μ M + 10 μ M). (B) WB analysis of HIF1 α and MYC protein expression in DLBCL patient-derived xenograft (PDX) models grown in normoxia (21% O₂) or hypoxia (5% O₂) for 16h and exposed to DMSO or F+R. (C) VEGFA secretion (enzyme-linked immunosorbent assay [ELISA] - conditioned media) in DLBCL cell lines grown in hypoxia (5% O₂) and exposed to F+R or DMSO for 16h. Data shown are mean \pm SD from three biological replicates. (D) VEGFA secretion (ELISA - conditioned media) in DLBCL PDX models grown in hypoxia (5% O₂) and exposed to F+R or vehicle control (DMSO). Data shown are mean \pm SD of three technical replicates; additional biological replicates are shown in Figure S4E. (E) Left panel - WB analysis of HIF1 α and MYC protein expression in HIF1 α wild-type (WT) or knockout (KO) SU-DHL10 cells grown in normoxia (21% O₂) or hypoxia (5% O₂) and exposed to DMSO or F+R; right panel - quantification of VEGFA suppression following exposure to F+R in HIF1 α WT or KO cells grown in hypoxia (data shown are VEGFA levels in conditioned media of DMSO minus VEGFA levels in F+R-treated cells, i.e., cAMP-mediated VEGFA clearance); full data in Figure S4I; data shown are mean \pm SD of three biological replicates. (F) left panel - WB analysis of HIF1 α and MYC expression in DLBCL cell lines exposed to DMSO, molidustat (prolyl hydroxylase inhibitor [PHDi], 10 μ M), or PHDi (10 μ M) + F+R for 16h in normoxia; right panel - VEGFA secretion (ELISA - conditioned media) in DLBCL cell lines exposed to molidustat (PHDi, 10 μ M), or PHDi (10 μ M) + F+R for 16h in normoxia. Data shown are mean \pm SD of three biological replicates. The *p* values in C–F are from two-sided Student's *t*-tests, **p* < 0.05, ***p* < 0.01, ****p* < 0.001, *****p* < 0.0001

PDE4 activity regulates both the tumour cell and TME to influence lymphoma angiogenesis

Recently, we created a compound E μ -Myc;Pde4b^{-/-} mouse and showed that B-cell lymphomas that develop in these

mice have suppressed angiogenesis.⁸ In this earlier work, we showed that Pde4b KO increased intracellular cAMP in the lymphoma cells, and suppressed VEGFA secretion in the TME.⁸ However, the cAMP/PDE4 axis has also been suggested to directly influence endothelial cells and inhibit vessel development in non-cancer models.^{13–16} Thus, to map

all cAMP anti-angiogenic effects during lymphomagenesis, and to differentiate its non-cell and cell autonomous effects, we developed an adoptive transfer model with lymphomas derived from E μ -Myc mice. In this model, Pde4b was alternatively deleted (KO) in the B-cell lymphoma and/or in the recipient mice. Four cohorts were created: (i) Pde4b WT E μ -Myc B-cell lymphoma transplanted in WT recipient mice (WT-WT pairing); (ii) Pde4b WT E μ -Myc B-cell lymphoma transplanted in Pde4b KO recipient mice (WT-KO pairing); (iii) Pde4b KO E μ -Myc B-cell lymphoma transplanted in WT recipient mice (KO-WT pairing); (iv) Pde4b KO E μ -Myc B-cell lymphoma transplanted in Pde4b KO recipient mice (KO-KO pairing). Once enlarged lymph nodes were clinically detected, the mice were humanely killed, cervical lymph nodes collected and processed for histopathological and immunohistochemical analyses. Lymphoma diagnosis was confirmed in all cases, and MVD quantification performed as described.⁸ Pde4b WT lymphomas that developed in Pde4b WT mice (WT-WT) displayed significantly higher MVD than lymphomas arising from any of the other combinations (Figure 5A). Deletion of Pde4b exclusively in the recipient mouse (WT-KO) or in the lymphoma cell (KO-WT) had similar impact in angiogenesis suppression, whereas

double deletion of Pde4b, in the lymphoma and endothelial cell (KO-KO), led to the most marked suppression in angiogenesis (Figure 5A). Of importance, because E μ -Myc lymphomas display genetic heterogeneity, we used multiple donor lymphomas in each cohort thus controlling for intrinsic tumour aggressiveness as a potential confounding variable. This approach was validated by transplanting the same donor in genetically distinct recipient mice. In these instances, we found that Pde4b WT E μ -Myc B-cell lymphoma that developed in Pde4b KO mice displayed significantly fewer vessels than isogenic tumours that were transplanted in Pde4b WT mice (Figure 5B). Likewise, Pde4b KO E μ -Myc B-cell lymphoma that developed in Pde4b KO mice displayed less prominent angiogenesis than isogenic tumours transplanted in Pde4b WT mice (Figure 5B). We concluded that cAMP-PDE4 axis inhibits lymphoma angiogenesis by targeting the lymphoma cell and the TME.

DISCUSSION

In this report, we showed that MYC expression correlates with, and may contribute to, the degree of angiogenesis in

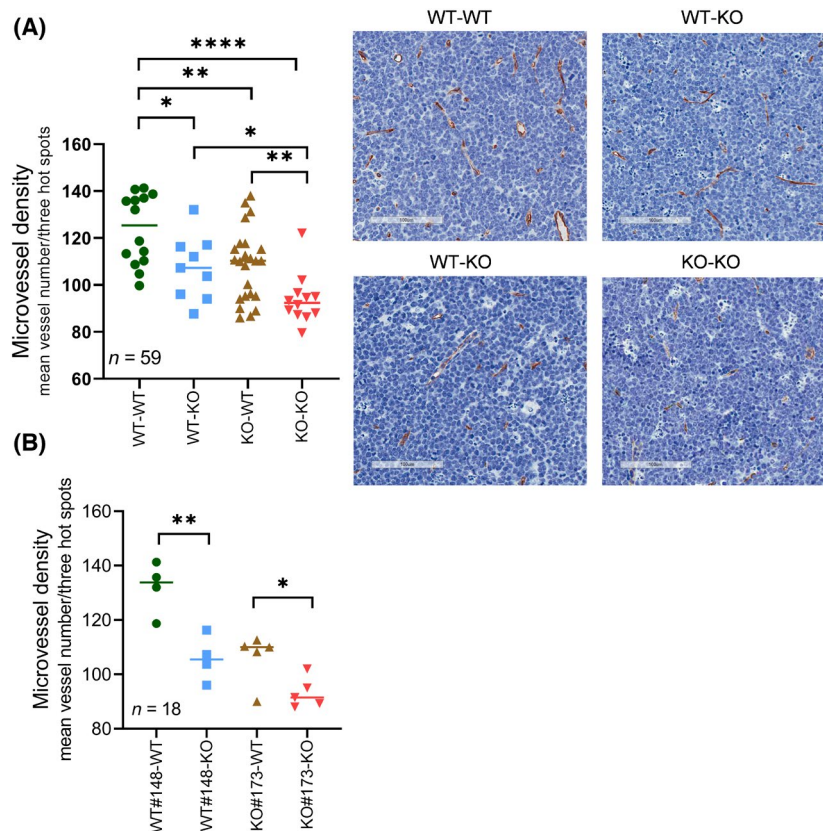


FIGURE 5 Differential phosphodiesterase 4b (Pde4b) expression in lymphoma or endothelial cells and angiogenesis in vivo. (A) Microvessel density (MVD) in Pde4b wild-type (WT) or Pde4b knockout (KO) B-cell lymphomas developing Pde4b WT or KO mice. Data shown are mean vessel number from three hot spots/tumour; each dot in the graph represents a unique tumour ($n = 59$). The p values are from two-sided unpaired Student's t -tests, * <0.05 , ** <0.01 , **** <0.0001 . Right panel shows representative CD34 immunohistochemistry of the four pairings shown in the graph; the size bar indicates 100 μ m. (B) MVD in lymphomas developing in Pde4b WT or Pde4b KO mice transplanted with the same donor lymphoma, either Pde4b WT (#148) or KO (#173) mice. Data shown are mean vessel number from three hot spots; each dot in the graph represents a unique tumour ($n = 18$). The p values are from two-sided unpaired Student's t -tests, * <0.05 , ** <0.01 .

DLBCL. We also demonstrated that this pro-angiogenic MYC activity can be blunted by modulation of the cAMP/PDE4 axis, *in vitro* and *in vivo*. This actionable node displays broad influence on lymphoma angiogenesis for it also inhibits HIF1 α expression during hypoxia. Although we had reported before on an interplay between cAMP/PDE4 signals and angiogenesis,⁸ here we established the broad mechanistic basis for these effects – MYC inhibition, HIF1 α suppression, and targeting of endothelial cells (summarised in Figure 6).

Despite the well-established role of MYC in angiogenesis,⁷ and in DLBCL pathogenesis,³ examination of this relationship has been limited to reports of a positive correlation between MYC expression and serum levels of VEGF,^{42,43} without direct vessel quantification in the lymphoma biopsy. We showed that MYC-positive DLBCL biopsies displayed significantly higher MVD and VEGF levels than MYC-negative lymphomas. This finding was not limited to DLBCLs dichotomised as MYC positive and negative (> or <40% positive cells by IHC) but rather had features of a continuous variable driving a positive correlation. The data from B cells from the E μ -Myc mouse model, DLBCL cell lines and PDX models analysed *in vitro* linked MYC expression and angiogenesis to VEGFA transcription and secretion. Of note, the importance of MYC as a mediator of cAMP inhibitory effects towards VEGFA was validated in MYC-null models, in which cAMP did not suppress VEGFA. These data suggest that an anti-angiogenic axis composed by cAMP-MYC-VEGFA is operational in B-cell lymphomas.

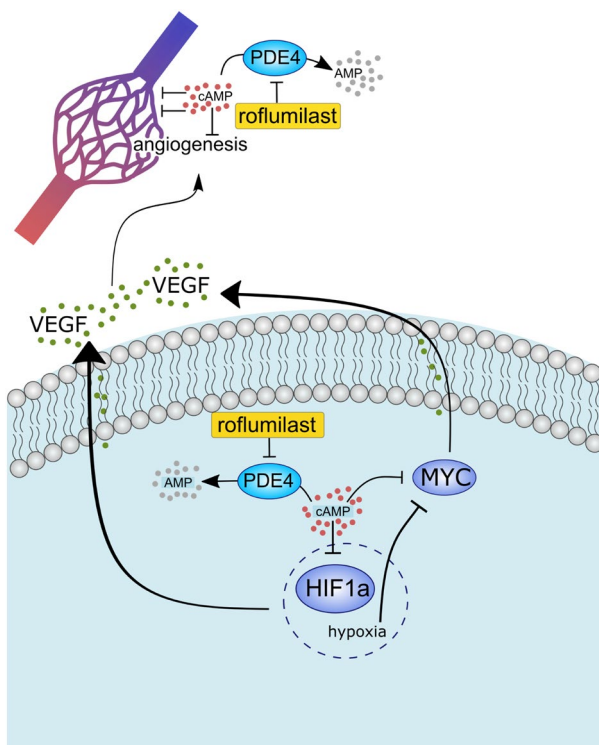


FIGURE 6 Graphic representation of the anti-angiogenic activities of the cyclic-AMP/phosphodiesterase 4 (cAMP/PDE4) axis

Analysis of large datasets of mature B-cell malignancies investigated by unbiased genome-wide gene expression methods, confirmed the relationship between MYC and VEGFA expression. These results suggest that the interplay between MYC, VEGF and angiogenesis, and possibly poor outcome, may be a common feature of B-cell tumours. Future examination of larger DLBCL series with parallel quantification of MYC expression and MVD will be important to validate these findings. Notably, although we have shown before that PDE4 inhibitors suppresses the growth and viability of DLBCL (reviewed in Cooney and Aguiar⁹) a concept that we have already tested in the clinic,⁴⁴ here we purposely used assays that avoided the confounding variables derived from the cAMP-PDE4-mediated cell growth suppression, and all output data were normalised by the number of cells at time of data collection. Thus, we are confident that the anti-angiogenic profile that we detected in our models are not a surrogate for cAMP-PDE4-driven growth inhibition.

The TME is a dynamic cellular milieu that often displays reduced oxygen availability, resulting in increased activity of HIFs, which in turn upregulate the expression of genes that promote angiogenesis, culminating in tumour survival and progression. Interruption of this cancer permissive cycle with anti-VEGF agents has been implemented with modest success in epithelial cancers but failed to provide benefit in DLBCL.^{4,45} Here, we provided data linking cAMP to HIF1 α and VEGFA in DLBCL. We found that cAMP transcriptionally represses HIF1 α during hypoxia, with attendant downregulation of multiple HIF1 α direct targets, including VEGFA. As hypoxia can independently repress MYC it became important to test the relevance of the putative cAMP-HIF1 α -VEGFA interplay. Examination of HIF1 α KO DLBCL model, as well as lymphomas with HIF1 α pharmacologically stabilised (i.e., exposed to PHD inhibitors), supported the concept that HIF1 α is, at least in part, mediating cAMP effects on VEGFA expression. Unexpectedly, we also found that contrary to earlier reports in epithelial cell models,^{40,41} in DLBCL the hypoxia-induced suppression of MYC is HIF1 α independent. Future studies are necessary to define which hypoxia-associated signals repress MYC in this tumour type.

In summary, we showed that MYC expression, at least in part via VEGFA expression/secretion, positively correlates with angiogenesis in DLBCL. In seeking to perturb this lymphogenic/pro-angiogenic signal with therapeutic intent, we found that modulation of cAMP levels could suppress lymphoma angiogenesis at least in part by repressing MYC, HIF1 α and the vascular endothelium.

ACKNOWLEDGEMENTS

This work was funded by grants from the National Institute of Health (R01-ES031522 and R01-GM140456), the Cancer Prevention and Research Institute of Texas (CPRIT - RP170146), the Veterans Administration (I01BX001882), and the Leukaemia and Lymphoma Society (TRP 6524-17), all to RCTA.

CONFLICT OF INTEREST

The authors declare that they have no competing interests.

AUTHOR CONTRIBUTIONS

Purushoth Ethiraj and Binu Sasi designed, performed, and interpreted the assays; An-Ping Lin, Zhijun Qiu, Carine Jaafar and Alia Elkhaili performed experiments; Parth Desai, Annapurna Saksena, Jacob P. Ritter and Kenneth N. Holder procured and characterised primary tumours, and performed pathological analyses; Ricardo C. T. Aguiar conceived the project, designed, and interpreted the assays, wrote manuscript, which was reviewed by all authors.

ORCID

Ricardo C. T. Aguiar  <https://orcid.org/0000-0002-8791-5849>

REFERENCES

- Cardesa-Salzman TM, Colomo L, Gutierrez G, Chan WC, Weisenburger D, Climent F, et al. High microvessel density determines a poor outcome in patients with diffuse large B-cell lymphoma treated with rituximab plus chemotherapy. *Haematologica*. 2011;96(7):996–1001.
- Stopeck AT, Unger JM, Rimsza LM, LeBlanc M, Farnsworth B, Iannone M, et al. A phase 2 trial of standard-dose cyclophosphamide, doxorubicin, vincristine, prednisone (CHOP) and rituximab plus bevacizumab for patients with newly diagnosed diffuse large B-cell non-Hodgkin lymphoma: SWOG 0515. *Blood*. 2012;120(6):1210–7.
- Butler MJ, Aguiar RCT. Biology informs treatment choices in diffuse large B cell lymphoma. *Trends Cancer*. 2017;3(12):871–82.
- Seymour JF, Pfreundschuh M, Trneny M, Sehn LH, Catalano J, Csinady E, et al. R-CHOP with or without bevacizumab in patients with previously untreated diffuse large B-cell lymphoma: final MAIN study outcomes. *Haematologica*. 2014;99(8):1343–9.
- Ennishi D, Hsi ED, Steidl C, Scott DW. Toward a new molecular taxonomy of diffuse large B-cell lymphoma. *Cancer Discov*. 2020;10(9):1267–81.
- Hsieh AL, Walton ZE, Altman BJ, Stine ZE, Dang CV. MYC and metabolism on the path to cancer. *Semin Cell Dev Biol*. 2015;43:11–21.
- Baudino TA, McKay C, Pendeville-Samain H, Nilsson JA, Maclean KH, White EL, et al. C-Myc is essential for vasculogenesis and angiogenesis during development and tumor progression. *Genes Dev*. 2002;16(19):2530–43.
- Suhasini AN, Wang L, Holder KN, Lin AP, Bhatnagar H, Kim SW, et al. A phosphodiesterase 4B-dependent interplay between tumor cells and the microenvironment regulates angiogenesis in B-cell lymphoma. *Leukemia*. 2016;30(3):617–26.
- Cooney JD, Aguiar RC. Phosphodiesterase 4 inhibitors have wide-ranging activity in B-cell malignancies. *Blood*. 2016;128(25):2886–90.
- Nam J, Kim DU, Kim E, Kwak B, Ko MJ, Oh AY, et al. Disruption of the Myc-PDE4B regulatory circuitry impairs B-cell lymphoma survival. *Leukemia*. 2019;33(12):2912–23.
- Pullamsetti SS, Banat GA, Schmall A, Szibor M, Pomagruc D, Hanze J, et al. Phosphodiesterase-4 promotes proliferation and angiogenesis of lung cancer by crosstalk with HIF. *Oncogene*. 2013;32(9):1121–34.
- Torii S, Okamura N, Suzuki Y, Ishizawa T, Yasumoto K, Sogawa K. Cyclic AMP represses the hypoxic induction of hypoxia-inducible factors in PC12 cells. *J Biochem*. 2009;146(6):839–44.
- Campos-Toimil M, Lugnier C, Droy-Lefaix MT, Takeda K. Inhibition of type 4 phosphodiesterase by rolipram and Ginkgo biloba extract (EGb 761) decreases agonist-induced rises in internal calcium in human endothelial cells. *Arterioscler Thromb Vasc Biol*. 2000;20(9):E34–40.
- Mendes JB, Rocha MA, Araujo FA, Moura SA, Ferreira MA, Andrade SP. Differential effects of rolipram on chronic subcutaneous inflammatory angiogenesis and on peritoneal adhesion in mice. *Microvasc Res*. 2009;78(3):265–71.
- Favot L, Keravis T, Holl V, Le Bec A, Lugnier C. VEGF-induced HUVEC migration and proliferation are decreased by PDE2 and PDE4 inhibitors. *Thromb Haemost*. 2003;90(2):334–43.
- Favot L, Keravis T, Lugnier C. Modulation of VEGF-induced endothelial cell cycle protein expression through cyclic AMP hydrolysis by PDE2 and PDE4. *Thromb Haemost*. 2004;92(3):634–45.
- Qiu Z, Lin AP, Jiang S, Elkashef SM, Myers J, Srikantan S, et al. MYC regulation of D2HGDH and L2HGDH influences the epigenome and Epitranscriptome. *Cell Chem Biol*. 2020;27(5):538–50.e7.
- Sasi B, Ethiraj P, Myers J, Lin AP, Jiang S, Qiu Z, et al. Regulation of PD-L1 expression is a novel facet of cyclic-AMP-mediated immunosuppression. *Leukemia*. 2020;35:1990–2001.
- Lin AP, Abbas S, Kim SW, Ortega M, Bouamar H, Escobedo Y, et al. D2HGDH regulates alpha-ketoglutarate levels and dioxygenase function by modulating IDH2. *Nat Commun*. 2015;6:7768.
- Lin AP, Qiu Z, Ethiraj P, Sasi B, Jaafar C, Rakheja D, et al. MYC, mitochondrial metabolism and O-GlcNAcylation converge to modulate the activity and subcellular localization of DNA and RNA demethylases. *Leukemia*. 2022;36(4):1150–9.
- Bouamar H, Jiang D, Wang L, Lin AP, Ortega M, Aguiar RC. MicroRNA 155 control of p53 activity is context dependent and mediated by Aicda and Socs1. *Mol Cell Biol*. 2015;35(8):1329–40.
- Jiang D, Aguiar RC. MicroRNA-155 controls RB phosphorylation in normal and malignant B lymphocytes via the noncanonical TGF-beta1/SMAD5 signaling module. *Blood*. 2014;123(1):86–93.
- Swerdlow SH, Campo E, Pileri SA, Harris NL, Stein H, Siebert R, et al. The 2016 revision of the World Health Organization classification of lymphoid neoplasms. *Blood*. 2016;127(20):2375–90.
- Hans CP, Weisenburger DD, Greiner TC, Gascoyne RD, Delabie J, Ott G, et al. Confirmation of the molecular classification of diffuse large B-cell lymphoma by immunohistochemistry using a tissue microarray. *Blood*. 2004;103(1):275–82.
- Hu S, Xu-Monette ZY, Tzankov A, Green T, Wu L, Balasubramanyam A, et al. MYC/BCL2 protein coexpression contributes to the inferior survival of activated B-cell subtype of diffuse large B-cell lymphoma and demonstrates high-risk gene expression signatures: a report from the international DLBCL rituximab-CHOP consortium program. *Blood*. 2013;121(20):4021–31. quiz 250.
- Green TM, Young KH, Visco C, Xu-Monette ZY, Orazi A, Go RS, et al. Immunohistochemical double-hit score is a strong predictor of outcome in patients with diffuse large B-cell lymphoma treated with rituximab plus cyclophosphamide, doxorubicin, vincristine, and prednisone. *J Clin Oncol*. 2012;30(28):3460–7.
- Johnson NA, Slack GW, Savage KJ, Connors JM, Ben-Neriah S, Rogic S, et al. Concurrent expression of MYC and BCL2 in diffuse large B-cell lymphoma treated with rituximab plus cyclophosphamide, doxorubicin, vincristine, and prednisone. *J Clin Oncol*. 2012;30(28):3452–9.
- Salven P, Orpana A, Teerenhovi L, Joensuu H. Simultaneous elevation in the serum concentrations of the angiogenic growth factors VEGF and bFGF is an independent predictor of poor prognosis in non-Hodgkin lymphoma: a single-institution study of 200 patients. *Blood*. 2000;96(12):3712–8.
- Gomez-Gelvez JC, Salama ME, Perkins SL, Leavitt M, Inamdar KV. Prognostic impact of tumor microenvironment in diffuse large B-cell lymphoma uniformly treated with R-CHOP chemotherapy. *Am J Clin Pathol*. 2016;145(4):514–23.
- Norrby K, Ridell B. Tumour-type-specific capillary endothelial cell stainability in malignant B-cell lymphomas using antibodies against CD31, CD34 and factor VIII. *APMIS*. 2003;111(4):483–9.
- Korkolopoulou P, Thymara I, Kavantzias N, Vassilakopoulos TP, Angelopoulou MK, Kokoris SI, et al. Angiogenesis in Hodgkin's lymphoma: a morphometric approach in 286 patients with prognostic implications. *Leukemia*. 2005;19(6):894–900.

32. de Bont ES, Rosati S, Jacobs S, Kamps WA, Vellenga E. Increased bone marrow vascularization in patients with acute myeloid leukaemia: a possible role for vascular endothelial growth factor. *Br J Haematol.* 2001;113(2):296–304.
33. Lenz G, Wright G, Dave SS, Xiao W, Powell J, Zhao H, et al. Stromal gene signatures in large-B-cell lymphomas. *N Engl J Med.* 2008;359(22):2313–23.
34. Liapis K, Clear A, Owen A, Coutinho R, Greaves P, Lee AM, et al. The microenvironment of AIDS-related diffuse large B-cell lymphoma provides insight into the pathophysiology and indicates possible therapeutic strategies. *Blood.* 2013;122(3):424–33.
35. Cerami E, Gao J, Dogrusoz U, Gross BE, Sumer SO, Aksoy BA, et al. The cBio cancer genomics portal: an open platform for exploring multidimensional cancer genomics data. *Cancer Discov.* 2012;2(5):401–4.
36. Smith PG, Wang F, Wilkinson KN, Savage KJ, Klein U, Neuberg DS, et al. The phosphodiesterase PDE4B limits cAMP-associated PI3K/AKT-dependent apoptosis in diffuse large B-cell lymphoma. *Blood.* 2005;105(1):308–16.
37. Kim SW, Rai D, McKeller MR, Aguiar RC. Rational combined targeting of phosphodiesterase 4B and SYK in DLBCL. *Blood.* 2009;113(24):6153–60.
38. Kim SW, Rai D, Aguiar RC. Gene set enrichment analysis unveils the mechanism for the phosphodiesterase 4B control of glucocorticoid response in B-cell lymphoma. *Clin Cancer Res.* 2011;17(21):6723–32.
39. Cooney JD, Lin AP, Jiang D, Wang L, Suhasini AN, Myers J, et al. Synergistic targeting of the regulatory and catalytic subunits of PI3Kdelta in mature B-cell malignancies. *Clin Cancer Res.* 2018;24(5):1103–13.
40. Zhang H, Gao P, Fukuda R, Kumar G, Krishnamachary B, Zeller KI, et al. HIF-1 inhibits mitochondrial biogenesis and cellular respiration in VHL-deficient renal cell carcinoma by repression of C-MYC activity. *Cancer Cell.* 2007;11(5):407–20.
41. Wong WJ, Qiu B, Nakazawa MS, Qing G, Simon MC. MYC degradation under low O₂ tension promotes survival by evading hypoxia-induced cell death. *Mol Cell Biol.* 2013;33(17):3494–504.
42. Aref S, Mabed M, Zalata K, Sakrana M, El Askalany H. The interplay between c-Myc oncogene expression and circulating vascular endothelial growth factor (sVEGF), its antagonist receptor, soluble Flt-1 in diffuse large B cell lymphoma (DLBCL): relationship to patient outcome. *Leuk Lymphoma.* 2004;45(3):499–506.
43. Sang W, Zhou H, Qin Y, Shen Z, Yan D, Sun C, et al. Risk stratification model based on VEGF and international prognostic index accurately identifies low-risk diffuse large B-cell lymphoma patients in the rituximab era. *Int J Hematol.* 2021;114(2):189–98.
44. Kelly K, Mejia A, Suhasini AN, Lin AP, Kuhn J, Karnad AB, et al. Safety and pharmacodynamics of the PDE4 inhibitor roflumilast in advanced B-cell malignancies. *Clin Cancer Res.* 2017;23(5):1186–92.
45. Eelen G, Treps L, Li X, Carmeliet P. Basic and therapeutic aspects of angiogenesis updated. *Circ Res.* 2020;127(2):310–29.

SUPPORTING INFORMATION

Additional supporting information may be found in the online version of the article at the publisher's website.

How to cite this article: Ethiraj P, Sasi B, Holder KN, Lin A-P, Qiu Z, Jaafar C, Cyclic-AMP signalling, MYC and hypoxia-inducible factor 1 α intersect to regulate angiogenesis in B-cell lymphoma. *Br J Haematol.* 2022;00:1–11. <https://doi.org/10.1111/bjh.18196>